Molecular Crystals and Liquid Crystals Science and Technology. Section A. Molecular Crystals and Liquid Crystals
Publication details, including instructions for authors and subscription information:
http://www.tandfonline.com/loi/gmcl19

Evolution and Switching Dynamics of Solitary Spots in Nonlinear Optical Feedback Systems

M. Kreuzer [a], A. Schreiber [a] & B. Thüring [a]
[a] Institute of Applied Physics, Technische Hochschule Darmstadt, Germany

Version of record first published: 24 Sep 2006.

To cite this article: M. Kreuzer , A. Schreiber & B. Thüring (1996): Evolution and Switching Dynamics of Solitary Spots in Nonlinear Optical Feedback Systems, Molecular Crystals and Liquid Crystals Science and Technology. Section A. Molecular Crystals and Liquid Crystals, 282:1, 91-105

To link to this article: http://dx.doi.org/10.1080/10587259608037570

Mol. Cryst. Liq. Cryst., 1996, Vol. 282, pp. 91–105
Reprints available directly from the publisher
Photocopying permitted by license only

EVOLUTION AND SWITCHING DYNAMICS OF SOLITARY SPOTS IN NONLINEAR OPTICAL FEEDBACK SYSTEMS

M. KREUZER, A. SCHREIBER AND B. THÜRING
Institute of Applied Physics, Technische Hochschule Darmstadt, Germany

Abstract We have studied experimentally and numerically spontaneous transvere pattern formation in a single feedback experiment using an optically addressable liquid crystal light valve in the polarization mode as a nonlinear optical element. Scaling behaviour has been found and transitions between different types of patterns have been observed which can be easily controlled by the bias voltage of the liquid crystal light valve. In a certain range of this control parameter we have investigated the evolution of bright solitary spots showing noncritical slowing down in the switching characteristics. This dynamical behaviour is related to the existence of an unstable branch which separates the basins of attraction of two stable states.

INTRODUCTION

After the first experimental success of optical bistability in 1974 (for an overview see reference 1) the interest in nonlinear optical feedback system has increased very rapidly. New optically nonlinear materials and new concepts for its applications in digital optical information processing have stimulated a lot of theoretical and experimental investigations on optically bistable elements in the early 1980s.[1] On the other hand the predictions of dynamic instabilities in such elements – usually consisting of a nonlinear material inside the cavity of an optical resonator – with periodic oscillations, period doubling and deterministic chaos[2] have shown that nonlinear optical feedback systems can be very attractive models to study the fascinating dynamics of nonlinear systems. But at least the transversal effects due the strong spatial coupling of propagating optical waves, which tend to create spatial instabilities with spontaneous symmetry breaking, have led to a new field of interest in nonlinear optical feedback system: the phenomena of spontaneous transversal pattern formation.[3–6] The simple single feedback system proposed by Firth et.al.[7,8], where an optical wave passes through a thin slice of a dispersive nonlinear optical material and (after propagation over a distance L) is reflected back onto the material, as well as his predictions of the evolution of hexagonal patterns has stimulated a lot of experimental investigations with various nonlinear optical materials.[9–16] However, the nonlinear response of most nonlinear materials is very small, so that laser power is often a limiting factor in experimental investigations.

In most experiments only small–aperture patterns, where the aspect ratio between the laser beam diameter and the smallest structure of the pattern is very small, could be realized which are therefore strongly influenced by the boundary conditions of the incident beam. In this sense, optically addressable liquid crystal light valves (LCLV) as hybrid nonlinear optical elements with high modulation sensitivity and large space–bandwidth product have successfully expanded the variety of available materials. These devices were used as dispersive nonlinear material of the Kerr-type to study the onset of pattern formation[14], often including geometrical transformations like rotations in the feedback loop.[15,16]

The theoretical investigations of scaling laws in such feedback systems[7] have shown that the typical pattern wavelength λ_p usually scales with the square root of the propagation length L ($\lambda_p \propto \sqrt{L}$). On the other hand a nonlinear stability analysis and numerical simulations show that – if the nonlinearity is of the Kerr-type – the type of pattern is limited to stable positive hexagons while e.g. solutions like rolls and negative hexagons are unstable. In the mode of pure phase modulation LCLVs are usually assumed to be nonlinear elements of the Kerr-type and various experiments[14,17] have proved the theoretical predictions. A more realistic modelling of LCLVs including threshold and saturation effects has shown that also a hexagon–roll transition as well as negative hexagons should occur[18] like in single feedback experiments with sodium vapour as nonlinear optical material (non–Kerr type nonlinearity[12]).

A more complex and therefore fascinating situation is predicted if the LCLV is used in the polarization mode.[18] In this mode the system has a lot of formal similarities to dispersive nonlinear ring resonators. Therefore, also optical bistability and related phenomena should be observable. In this paper we present experimental results on pattern formation and scaling behaviour in such experiments. After a short theoretical description the experimental observations of various kind of stable patterns are presented. In the next section an important special phenomenon which is related to optical bistability is investigated in detail: the evolution and switching dynamics of solitary spots. Some experimental observations[6,19] as well as theoretical investigations[20,21] proposed recently give hints that complex patterns could be described by the interaction of solitary spots (sometimes called localized structures, 2-dimensional spatial solitons or optical bullet–holes) just like hexagonal patterns as closely packed solitary spots. Also, the transition to turbulent patterns may be described in this framework. With all respect, an interesting aspect is a possible formal analogy to hydrodynamics as well as chemical reactions.[22–25]

EXPERIMENTAL SETUP

Figure 1 displays the experimental setup we have used. The collimated and expanded beam of a linearly polarized frequency–doubled cw Nd:YAG–laser ($\lambda = 532\,\text{nm}$, max. power $\approx 100\,\text{mW}$) passes through the first beamsplitter and falls onto the read-out side of an optically addressable liquid crystal light valve (LCLV) under normal incidence. The other part of the beam is focused onto a monitor photodiode to detect the incident power of the laser beam which is controlled by an acousto-optic-modulator.

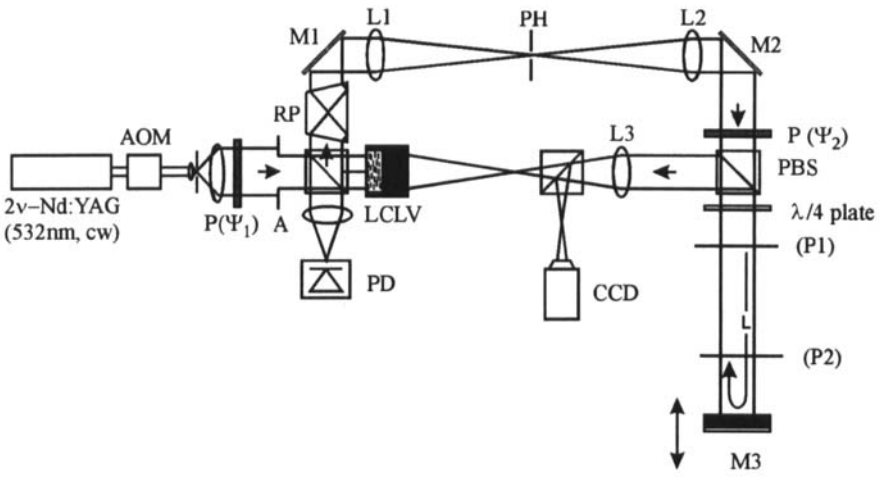

Figure 1: Experimental setup of the single feedback system using an optically addressable liquid crystal light valve (LCLV) in the polarization mode.

The LCLV as a nonlinear optical element with a planar oriented liquid crystal layer is working in the reflective mode. A bias voltage V_{ext} is applied to the sandwich structure of the read-out side and the write side of the LCLV. The read-out side is formed by the liquid crystal layer and a dielectric mirror, while a light blocking layer and the photoconducting layer act as the write side. Light incident on the write side of the the LCLV creates free charge carriers in the photoconducting layer resulting in a decrease of its impedance. The applied bias voltage, which now drops at the liquid crystal layer, reorients the liquid crystal molecules corresponding to the intensity distribution at the write side.

Working in the polarization mode, a $\lambda/2$-retarder plate $P(\Psi_1)$ adjust the angle Ψ_1 between the plane of polarization and the director of the liquid crystal molecules while the polarizer $P(\Psi_2)$ (orientation angle Ψ_2 with respect to the director) in the feedback loop converts the polarization modulation of the propagating beam into an amplitude modulation. The feedback loop itself is set up by the first beam splitter, the two mirrors M1 and M2, the polarizing beam splitter PBS, and the mirror M3. The rotating prism RP and the lenses L1 and L2 give an 1:1 imaging of the LCLV read-out side onto the image plane P1. From P1 the feedback wave propagates freely until reaching plane P2, which is the object plane of lens L3. This lens images the intensity distribution at P2 onto the write side of the LCLV (note that all reflections and the imaging result in an effective propagation of the wave without any residual rotation of the beam). In this way propagation effects (phase–amplitude transformations by diffraction) effectively take places only between the planes P1 and P2. The mirror M3 is mounted on a computer–controlled translation stage, allowing for simple and precise control of the length of free space propagation L. The LCLV itself is a self–defocusing nonlinearity (the effective refractive index of the LC-layer decreases with an increase of the intensity on the

write side). If the object plane P2 is put in front of plane P1, we can experimentally simulate a self–focusing nonlinearity.[18,26] In the feedback loop the lenses L1 and L2 together with the pinhole PH form a spatial low–pass filter which controls the spatial resolution of the system. A CCD camera, positioned in the image plane of lens L3, detects the intensity distribution of the feedback wave and is connected to a video cassette recorder and a PC–based image processing system.

THEROTICAl MODEL

For the theoretical description of our single feedback system we consider the simplified scheme shown in figure 2. The angle Ψ_1 between the plane of polarization of

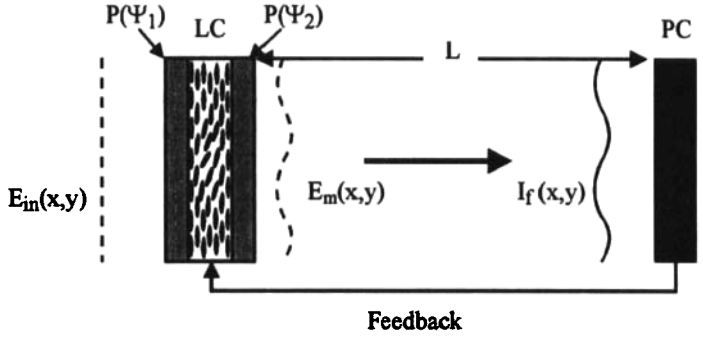

Figure 2: Simplified scheme of the feedback system. The LCLV is unfolded into the liquid crystal layer and the photoconducting layer (see text).

the incident linearly polarized field distribution E_{in} and the director of the planar oriented layer is adjusted by a half-wave plate. Passing through the liquid crystal layer the extraordinary beam suffers an additional phase shift ϕ. Using a continuum ansatz for the reorientation of the liquid crystal molecules in an external field this phase difference between the ordinary and extraordinary beam can be described by the following material equation[18]

$$\tau\frac{\partial}{\partial t}\phi - l^2\nabla_\perp^2\phi + \phi = \phi_{\max}\begin{cases} 1 & for \quad (\mu_s I_w + J_b) < 0 \\ 1-\tanh^2(\mu_s I_w + J_b) & for \quad (\mu_s I_w + J_b) \geq 0, \end{cases} \tag{1}$$

where τ is the relaxation time, l is an effective diffusion length describing the elastic coupling inside the liquid crystal as well as carrier diffusion in the photconducting layer, $\nabla_\perp^2 = \frac{\partial^2}{\partial x^2} + \frac{\partial^2}{\partial y^2}$ is the transverse Laplacian, $\phi_{\max}$ is the maximum possible phase difference, μ_s is a modulation sensitivity and I_w is the intensity distribution at the write side of the photoconducting layer (PC). The rhs of eq. (1) includes threshold and saturation effects which are determined by a 'bias intensity' J_B. This bias intensity is related to the voltage V_{ext} by the relations

$$\mu_s \equiv \frac{\kappa_i V_{\text{ext}}}{V_0}, \qquad J_b \equiv \frac{\kappa_d V_{\text{ext}} - V_{th}}{V_0}, \tag{2}$$

where V_{th} is the threshold voltage and κ_d, κ_i and V_o are constants which depend on the properties of the LCLV. After passing the LC-layer the polarization modulation is transformed by the polarizer $P(\Psi_2)$ (orientation angle Ψ_2 with respect to the director) into an amplitude modulation:

$$\vec{E}_m = (\vec{B}e^{i\phi} + \vec{C})E_{\text{in}} \tag{3}$$

where the vectors $\vec{B}$ and $\vec{C}$

$$\vec{B} = \cos\Psi_1 \cos\Psi_2 \begin{pmatrix} \cos\Psi_2 \\ \sin\Psi_2 \end{pmatrix}, \quad \vec{C} = \sin\Psi_1 \sin\Psi_2 \begin{pmatrix} \cos\Psi_2 \\ \sin\Psi_2 \end{pmatrix} \tag{4}$$

can be obtained using the Jones calculus.[18] After passing the liquid crystal layer the free propagation of the wave E_m onto the photo conducting layer can be approximated by the stationary scalar paraxial wave equation

$$\nabla_\perp^2 E - 2\mathrm{ik}\frac{\partial}{\partial z}E = 0, \tag{5}$$

where k is the wave number of the light field. The formal solution of eq. (5) for the wave propagation over the distance L is

$$E_f = e^{-i(L/2k)\nabla_\perp^2}\{E_m\}, \tag{6}$$

which results in the feedback intensity distribution I_w at the photoconducting layer

$$I_w = I_f \equiv |E_f|^2 = |e^{-i(L/2k)\nabla_\perp^2}\{(Be^{-i\phi} + C)E_{in}\}|^2 \,. \tag{7}$$

PATTERN FORMATION

Eqn. (1) and (7) describe the spatio–temporal behaviour of our feedback system. In a first approach we will have a short look at the stationary and spatially homogeneous solution ($\frac{\partial}{\partial t} = 0 = \nabla_\perp^2$) assuming a plane input wave. For this case we get

$$I_f = \left(B^2 + C^2 + 2BC\cos\phi^{(o)}\right) I_{in} = \alpha\left(1 + \gamma\cos\phi^{(o)}\right) I_{in} \tag{8}$$

$$\phi^{(o)} = \phi_{\max}(1 - \tanh^2(\mu_s I_f + J_b)) \tag{9}$$

with the substitutions

$$\begin{aligned} \alpha &= B^2 + C^2 = \frac{1}{2}\left(\cos^2(\Psi_1 - \Psi_2) + \cos^2(\Psi_1 + \Psi_2)\right) \\ \beta &= \frac{2B^2}{\alpha} = \frac{(\cos(\Psi_1 - \Psi_2) + \cos(\Psi_1 + \Psi_2))^2}{\cos^2(\Psi_1 - \Psi_2) + \cos^2(\Psi_1 + \Psi_2)} \\ \gamma &= \frac{2BC}{\alpha} = \frac{(\cos^2(\Psi_1 - \Psi_2) - \cos^2(\Psi_1 + \Psi_2)}{(\cos^2(\Psi_1 - \Psi_2) + \cos^2(\Psi_1 + \Psi_2)} \,. \end{aligned} \tag{10}$$

For a given setting of the angles Ψ_1 and Ψ_2 and a fixed value of the maximum achievable phase shift $\phi_{\max}$, which is given by the properties of our LCLV to be $\phi_{\max} = 6\pi$, the transfer characteristics of the system depends only on the control parameter J_b. Except for the case $\Psi_1 = \Psi_2 = 0$, which corresponds to the case of pure phase modulation, the system shows differential gain and/or multistability. As mentioned above, the solutions for the system show formal similarities to the behaviour of dispersive nonlinear ring resonators where the detuning phase from resonance corresponds to the 'bias intensity' J_b in our system. An experimental approximation of the situation dicussed above can be realized by putting the image plane P1 at the same position as the object plane P2 ($L = 0$).

The second approach is to study the stability of the homogeneous solution against small inhomogeneous distortions when free space propagation (diffraction) has to be taken into account ($L \neq 0$). A linear stability analysis for the system has been performed[18] to calculate the threshold of the input intensity where an unstable transverse wavenumber K occurs. The result is an equation for the critical exponent λ_p

$$\lambda_p = \frac{-2\phi_N\phi^{(0)}\left(\beta\sin(q^2) + \gamma\sin(q^2 - \phi^{(0)})\right)}{1 + \gamma\cos\phi^{(0)}}\left(\operatorname{arctanh}(\phi_N) - J_b\right) - l^2q^2 - 1 \quad (11)$$

with

$$q^2 = \frac{LK^2}{k} \qquad \text{and} \qquad \phi_N = \sqrt{1 - \frac{\phi^{(0)}}{\phi_{\max}}}\,.$$

When the critical exponent exceeds zero, a typical transverse wave number $|K_c|$ becomes unstable. From this implicit equation (11) for the threshold intensities I_{th} ($I_{\text{th}} = I_{\text{in}}(K, J_b)$ for $\lambda_p = 0$) one usually deduces the critical wave number $|K_c|$ which has the lowest threshold intensity. At this point one assumes that the homogeneous solution becomes unstable and a new output pattern spontaneously forms with a typical wavenumber $|K_c|$ while the type of pattern can not be predicted by the linear stability analysis.

Figure 3 displays the theoretical scaling behaviour in dependence on the 'bias intensity' J_b and the experimentally observed stationary pattern when the input intensity exceeds the threshold intensity (for $\Psi_1 = 40°$ and $\Psi_2 = 40°$, self-focusing case: $L = -18\,\text{cm}$). While the unstable wavenumber $|K_c|$ oscillates with increasing control parameter J_b, transitions between different patterns also occur.

At low 'bias intensities' solitary bright spots on arbitrary positions develop which switch in a smooth transition of a 'melting'–process to a pattern of negative hexagons. With further increasing of the control parameter, a negative hexagons – stripes (rolls) – positive hexagons transition is observed. At point (f) again localized spots were observed but now on a weak hexagonal net. We assume that the suppressing of this hexagonal net at low J_b can be explained by the threshold effect of the reorientation at low external voltages. The sequence of pattern transitions is periodically repeated until the reorientation of the liquid crystal layer saturates.

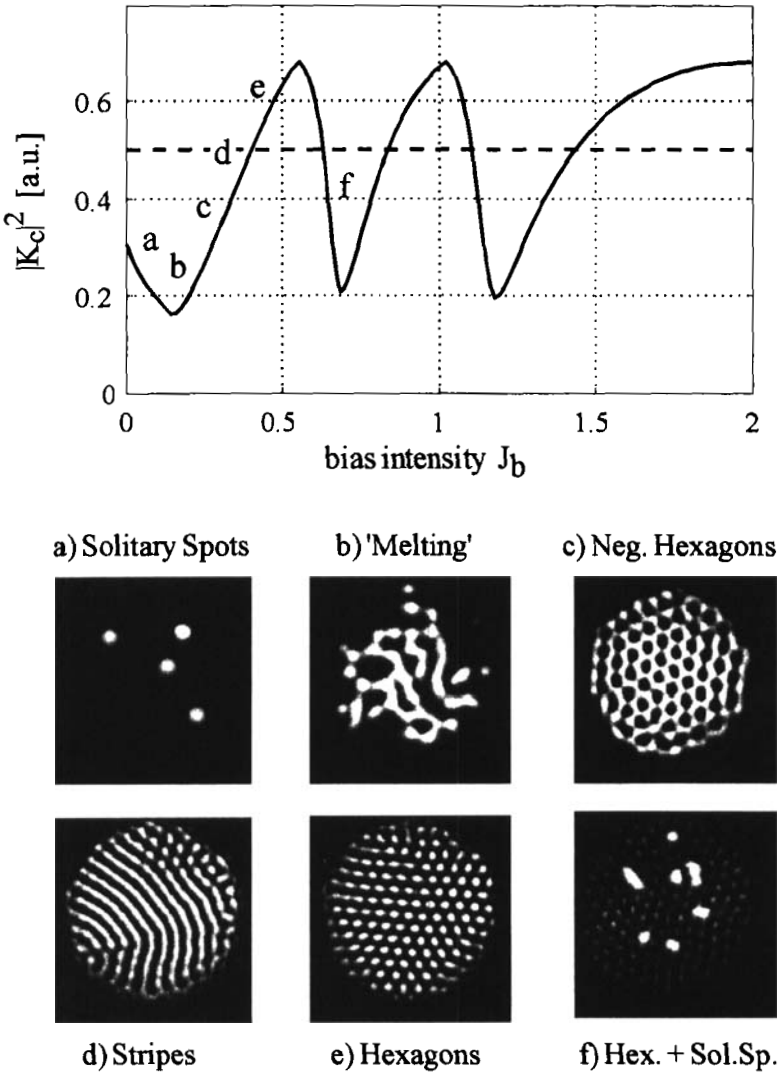

Figure 3: Top: Scaling behaviour of the most unstable pattern wavenumber $|K_c|$ as a function of the control parameter J_b (bias intensity $\hat{=}$ external voltage). The dashed line corresponds to the unstable wavenumber in the case of pure phase modulation. Bottom: Experimentally observed stationary near-field patterns. The input beam had a diameter $D \approx 6\,\mathrm{mm}$. With increasing bias intensity the pattern changes from solitary spots to negative hexagons H^-, stripes S, positive hexagons H^+ and to a coexistence of hexagons at the low branch and solitary spots. The behaviour is periodically repeated until the reorientation of the liquid crystal is saturated.

The transition between different types of pattern is a very interesting phenomenon and will be discussed elsewhere. In the following we will concentrate on the evolution and switching dynamics of the observed solitary spots.

SOLITARY SPOTS

Solitary spots like localized structures in hydrodynamics[22,23] or 'optical bullet holes' in nonlinear optical resonators[21,27] have been observed in various nonlinear systems. Besides the applications of solitary units for binary information encoding[28,29] they can be elementary processes describing the behaviour of full complex systems. In such cases, the evolution and spatio–temporal behaviour of complex systems can be approximated in terms of localized structures with lesser degree of freedom.[19,21,22]

The evolution of such bright spots or localized structures in nonlinear optical feedback systems can be motivated in the framework of classical optical bistability of the homogeneous solution. Let us consider the stationary solution of an optically

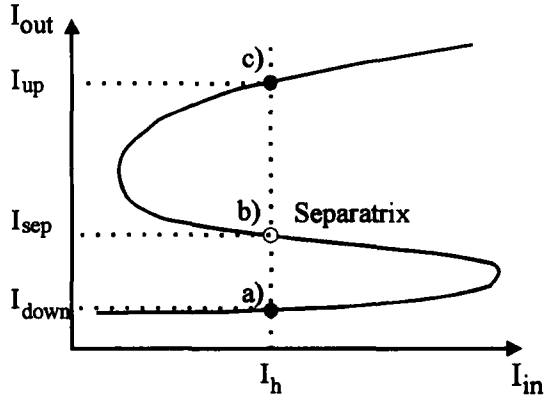

Figure 4: Hysteresis loop of the homogeneous solution of the feedback system. At the holding intensity I_h three sationary solutions for output intensity exist: a) I_{down}: low state (stable), b) I_{sep}: Separatrix (unstable) and c) I_{up}: high state (stable). The point b) is a point of the so-called separatrix which separates the basins of attraction of the two stable states.

bistable device shown in figure 4. The so-called separatrix, which is the unstable branch (with negative slope) separates the basins of attraction of the two stable branches. If the whole system is – illuminated by an constant cw holding intensity I_h – is on the lower branch and a locally restricted strong addressing pulse is applied to the system it can be locally switched onto the upper branch forming a bright spot. Transversal effects like selffocusing may be able to stabilize the spot so that it becomes a stable and robust solution.[19,20,30,31] An experimental proof of this simple explanation can be given by the investigation of the switching dynamics.

To investigate the dynamical behaviour and related phenomena in our system, we have modified the experimental setup shown in figure 1. As shown in the

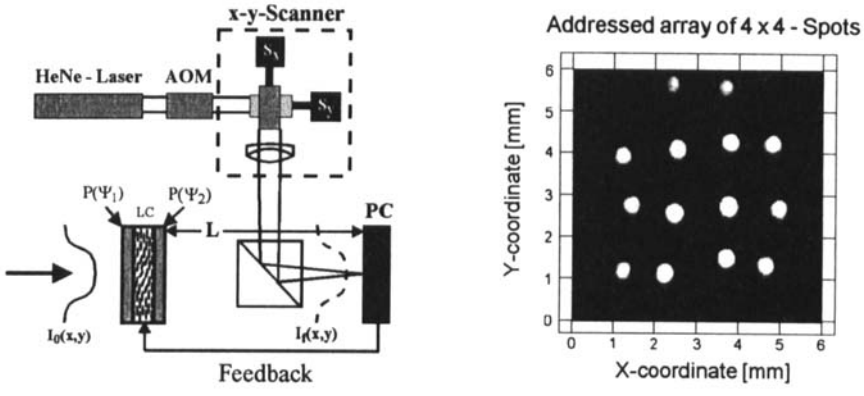

Figure 5: a) Principle of the external addressing scheme of solitary spots. A collimated beam of a HeNe-laser is scanned via two galvo-scanners and focused onto the writing side (photoconducting layer) of the LCLV. The intensity of the laser beam is modulated by an acusto-optic-modulator. b) Stationary pattern of an addressed array of solitary spots using a holding beam with diameter $D \approx 6\,\mathrm{mm}$.

scheme of the unfolded feedback loop (see figure 5a) we have used a second laser for the external addressing of solitary spots. Using an acousto–optic modulator and a xy–galvano–scanner system bright spots can be addressed independently in space and time. Starting from a dark homogeneous solution figure 5b shows the stationary result of an array of addressed solitary spots.

Switching Dynamics – Noncritical Slowing Down

Let us consider again the one-dimensional* bistable situation shown in figure 4. Corresponding to the constant holding intensity, which should be far away from the switching points, there exist three stationary states for the output: I_{down} (low transmission, stable), I_{sep} (unstable) and I_{up} (high transmission, stable). (In the following all intensities are normalized to the critical intensity). If a short rectangular addressing pulse of duration τ_p is applied to the system there exists a critical intensity I_c, which will switch the device precisely to the unstable separatrix. In absence of fluctuations the relaxation time Δt back to a stable configuration will diverge to infinity. If the intensity I_p of the address pulse differs from the critical intensity by a smallness parameter ε ($I_p = I_c + \varepsilon$) the system will switch either to the upper or lower branch depending on the sign of ε. The divergence of the switching time far from the switching points of the hysteresis loop is called noncritical slowing down. The relation between the decay time Δt and the strength of the seed ε for one-dimensional bistable devices was first predicted by Mandel et.

*This means zero-dimensional in space and one-dimensional in time, somtimes written as (0+1)–dimensional.

al.[32] and has been investigated in various experiments.[33,34]

In order to obtain an analytical result for the scaling of the switching time Δt we consider the dynamics of the induced phase shift ϕ_i in the Kerr–approximation neglecting transverse effects:

$$\tau\dot{\phi}_i + \phi_i = \mu_k I_f \qquad \text{with} \qquad I_f = \alpha\left[1 + \gamma\cos(\phi_i + \phi_{\max})\right] I_{\text{in}} \,. \tag{12}$$

Evaluating eqn. (12) to the second order of ϕ_i this leads to an equation of motion for the order parameter ϕ_i

$$\dot{\phi}_i = A\phi_i^2 + B\phi_i + C \tag{13}$$

with the substitutions

$$A = -\frac{\mu_k\alpha\gamma}{2\tau} I_{\text{in}} \,, \quad B = -\frac{1}{\tau} \,, \quad C = \frac{\mu_k\alpha I_{\text{in}}}{\tau}\left(1+\gamma\right) \,,$$

which is very similar to the dynamics of the systems governed by a single degree of freedom, where in a good approximation one can replace the whole bistability curve by a parabola in the vicinity of the switching point.[32]

The steady state solution of these equations gives the solution for the lower branch as well as for the separatrix

$$\phi_{\text{i,down}} = \frac{-B + \sqrt{B^2 - 4AC}}{2A} \quad \text{and} \quad \phi_{\text{i,sep}} = \frac{-B - \sqrt{B^2 - 4AC}}{2A} \tag{14}$$

while the solution for the upper branch recedes to infinity due to the evaluation mentioned above. For a detailed discussion of the solution for this differential equation (13) we refer to reference 32 and will discuss only the results for the lethargy time Δt. In contrast to the phenomena of critical slowing down at the switching points of the bistability curve, where the lethargy time scales with $\varepsilon^{-\frac{1}{2}}$, the switching times $\Delta t_\uparrow$ to the upper state and $\Delta t_\downarrow$ back to the lower state scale logarithmically with ε:

$$\Delta t_\uparrow, \Delta t_\downarrow \propto \ln|\varepsilon| \,. \tag{15}$$

This model developed for classical bistable optical elements in the plane wave limit has numerically proved to hold for localized states of a nonlinear cavity.[20] Here we present the first experimental results of noncritical slowing down of solitary spots in a single feedback experiment. Numerical simulations were performed using a Fourier transform algorithm to calculate free space propagation (eq. (5)) and a finite differences scheme to integrate the full material equation (1).

To create an addressing pulse of duration $\tau_p = 200\,\text{ms}$ and variable intensity I_P we used the setup shown in figure 5. The beam waist of the focused addressing beam had a gaussian intensity distribution and was adjusted to have approximately the same size as the spontaneously formed solitary spots observed in the experiments described in figure 3. The CCD camera in figure 1 was replaced by a photo diode detecting the dynamic behaviour of the total transmitted power. The area of the sensor was large enough to detect all relevant changes.

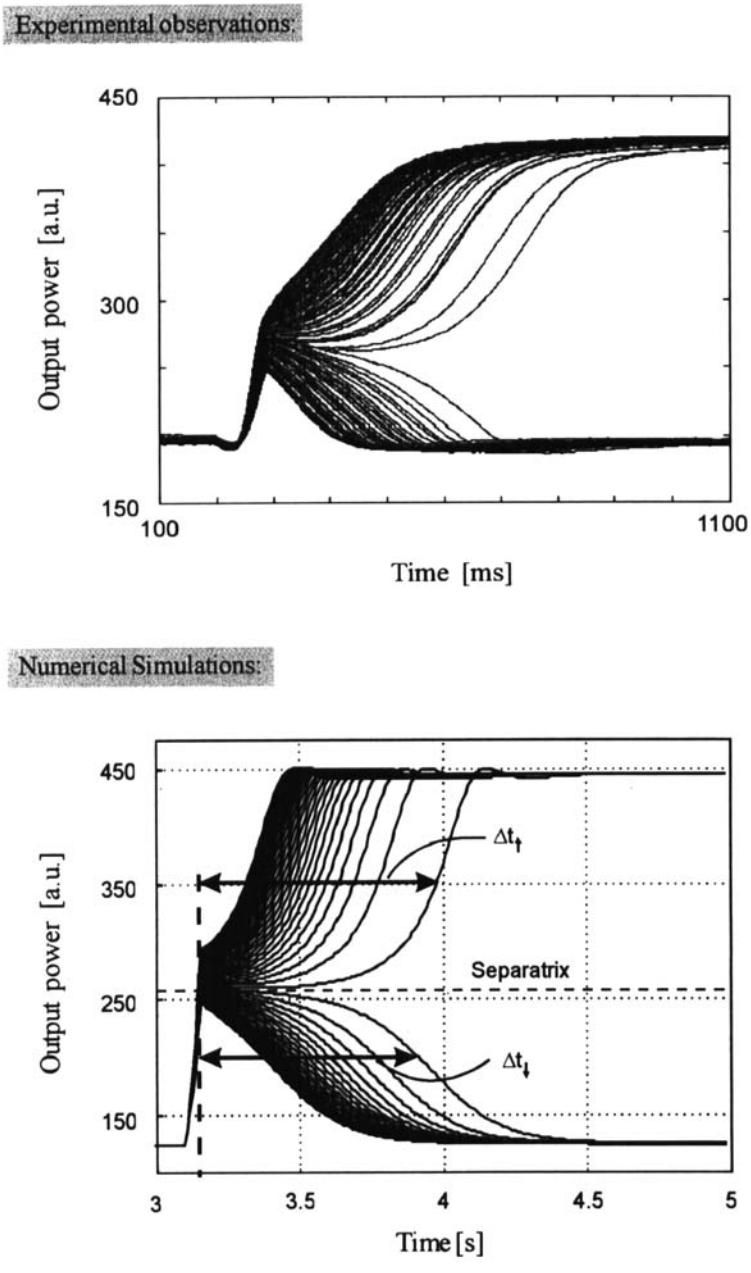

Figure 6: Switching dynamics of noncritical slowing down. At a constant holding intensity I_h far away from the turning points of the hysteresis loop a short pulse of the addressing beam with variable intensity I_p was applied. At low intensities I_p the system relaxes back to the low state. With increasing I_p the relaxation time $\Delta t_\downarrow$ increases until the system locally switches to the high state. With further increasing of I_p the switching time $\Delta t_\uparrow$ time decreases. Top: experimental observations; bottom: numerical simulations.

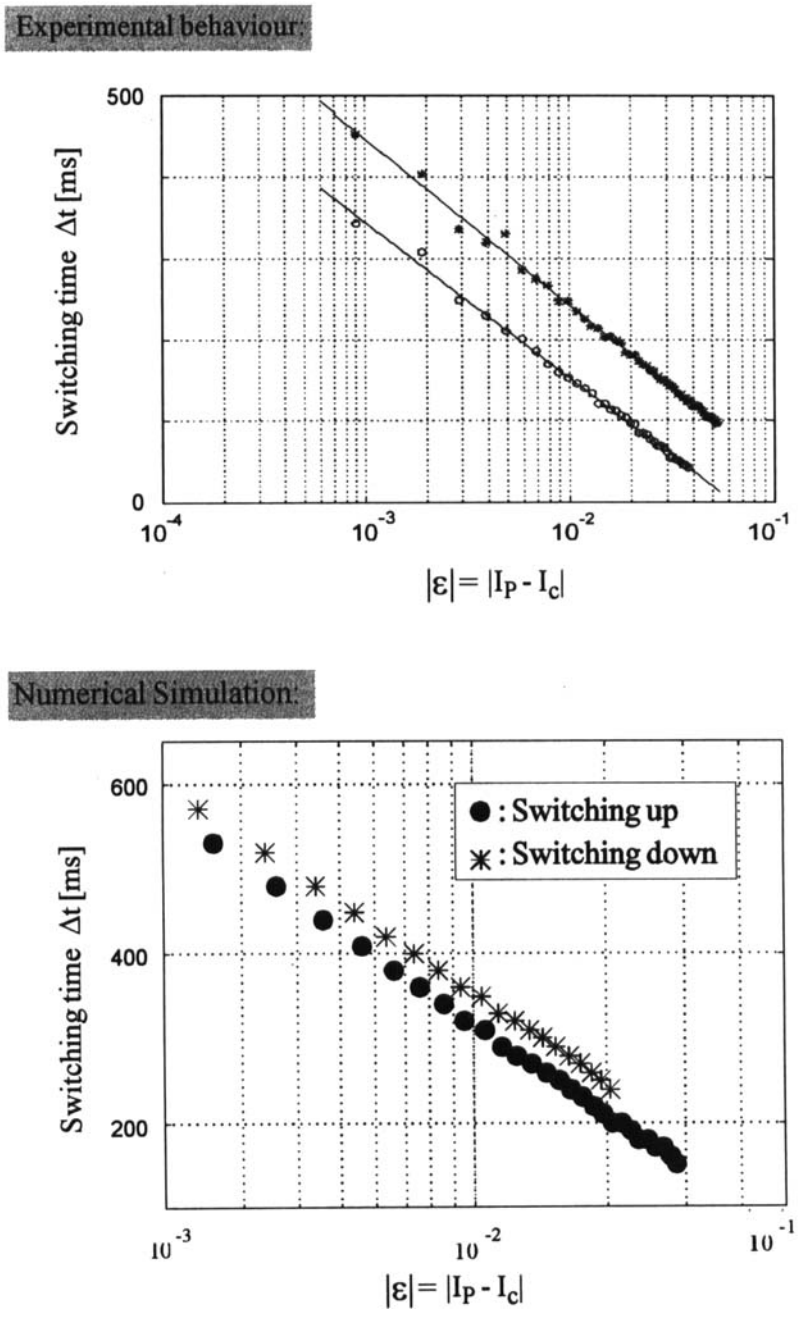

Figure 7: Switching times $\Delta t_\uparrow$ and relaxation times $\Delta t_\downarrow$ extracted from the results of figure 7 as a function of the overdrive amplitude $|\varepsilon| = |I_p - I_c|$. I_c is the critical intensity to switch exactly to the separatrix. Top: experimental observations; bottom: numerical simulations. The results agree with the predicted behaviour $\Delta t \propto \ln|\varepsilon|$.

Figure 6 shows the experimentally observed dynamical behaviour of the single feedback experiment in agreement with the numerical results. During the addressing pulse the system switches to an intermediate state in the neighbourhood of the unstable branch and relaxes back to a stable state after the end of the pulse. At low intensities $I_p < I_c$ the system relaxes back to the lower branch. Sucessively increasing the intensity I_p, the relaxation time $\Delta t_\downarrow$ – here defined as the time between the end of the addressing pulse and the 50% level between the separatrix and the stable end state – increases up to more than several orders of magnitude of the relaxation time ($\tau \approx 50$ ms) of the molecular reorientation. When I_p exceeds the critical intensity I_c, the system switches to the upper branch showing a decreasing switching time $\Delta t_\uparrow$ with increasing intensity I_p.

From these experiments we have extracted the switching times as a function of the overdrive amplitude ε. The experimental results as well as the results of the full numerical simulations (see figure 7) for the scaling behaviour of noncritical slowing down of solitary spots are quite the same as for one-dimensional optically bistable devices. This strengthens the denotion of the observed localized bright states as robust solitary spots.

We have verified this scaling behaviour for different holding intensities I_h. Usually the unstable branch separating the two basins of attraction is not accessible for experiments. But from each experiment (see e.g. figure 6 for a certain holding intensity) it is easy to reconstruct the corresponding point of the separatrix where the transition from relaxing to the lower branch to the switching to the upper branch appears. Figure 8 shows the reconstructed points from the

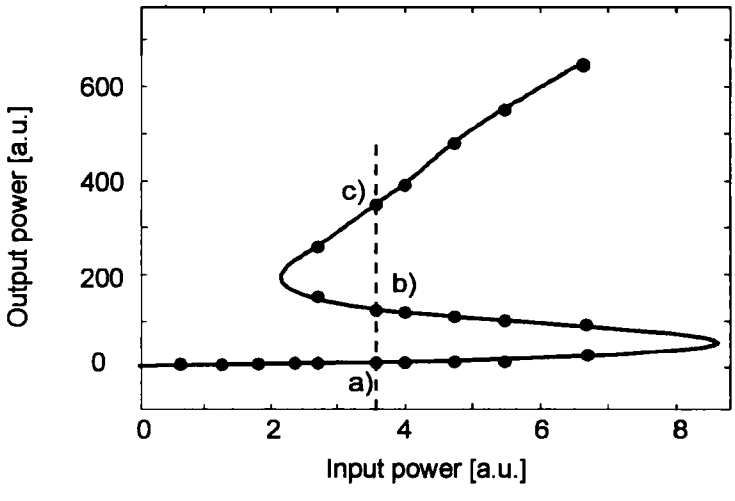

Figure 8: Reconstructed hysteresis loop of the stationary states of solitary structures in the single feedback system. The unstable states of the loop were obtained from measuring the separatrix for different holding intensities I_h.

experimental data for different holding intensities displaying the s–shaped curve of optical bistability.

SUMMARY

In conclusion we have shown experimental results on spontaneous pattern formation in a single feedback system using an optically addressable liquid crystal light valve as optical nonlinear material. Working in the polarization mode of the LCLV, various types of patterns and transitions between them could be observed, while the external voltage applied to the LCLV worked as a control parameter. In a certain parameter range the existance of bright solitary spots – which can appear on arbitrary locations in the space of the illuminated area – have been observed. These robust solitary spots have been described in the framework of optical bistability of localized structures. External addressing and noncritical slowing down in the switching dynamics of such localized states has been studied experimentally and numerically confirming the predicted behaviour.

We acknowledge stimulating discussions with R. Neubecker and G.-L. Oppo. This work has been supported by the Deutsche Forschungsgemeinschaft under the program "SFB 185 Nichtlineare Dynamik".

REFERENCES

1. H.M. Gibbs, Optical Bistability: Controlling Light with Light, (Academic Press, London, 1985).
2. K. Ikeda, H. Daido, and O. Akimoto, Phys. Rev. Lett., 45, 709–712 (1980).
3. N.B. Abraham and W.J. Firth (eds), Special issue: Transverse effects in nonlinear optical systems, (J. Opt. Soc. Am. B7, 1990).
4. L.A. Lugiato (ed), Special issue: Nonlinear optical structures, patterns, chaos, (Chaos, Solitons and Fractals, 4 (8/9), 1994).
5. M. Kreuzer, W. Balzer, and T.Tschudi, Appl.Opt., 29, 579–582 (1990).
6. M. Kreuzer, H. Gottschling, and T.Tschudi, Mol. Cryst. Liq. Cryst., 207, 219–230 (1991).
7. G. D'Alessandro and W.J. Firth, Phys.Rev. A, 46, 537–548 (1992).
8. W.J. Firth, J. Mod. Opt., 37, 151–153 (1990).
9. R. Macdonald and H.J. Eichler, Opt. Commun., 89, 289–295 (1992).
10. M. Tamburrini, M. Bonavita, and S. Wabnitz, Opt. Lett., 18, 855–857 (1993).
11. G. Grynberg, A. Maitre, and A. Petrossian, Phys. Rev. Lett., 72, 2379–2382 (1994).
12. T. Ackemann and W. Lange, Phys. Rev. A., 50, R1–R4 (1994).
13. J. Glueckstad and M. Saffmann, Opt. Lett., 20, 551–553 (1995).
14. B. Thüring, R. Neubecker, and T. Tschudi, Opt.Commun., 102, 111–115 (1993).
15. S.A. Akhmanov, M.A. Vorontsov, V.Yu. Ivanov, A.V. Larichev, and N.I. Zheleznykh, J. Opt. Soc. Am., B9, 78 (1992).
16. E. Pampoloni, S. Residori, and F.T. Arecchi, Europhys. Lett., 24, 647 (1993).

17. R. Neubecker, B. Thüring, and T. Tschudi, Chaos, Fractals and Solitons, 4, 1307–1321 (1994).
18. R. Neubecker, G.-L. Oppo, B. Thüring, and T. Tschudi, Phys. Rev. A, 52, 789–808 (1995).
19. M. Kreuzer, H. Gottschling, R. Neubecker, and T. Tschudi, Appl. Phys. B, 59, 581–589 (1994).
20. W.J. Firth and A.J. Scroggie, submitted to Phys. Rev. Lett., (1995).
21. M. Tlidi, P. Mandel, and R. Lefever, Phys. Rev. Lett., 73, 640–643 (1994).
22. S. Toh, H. Iwasaki, and T. Kawahara, Phys. Rev. A, 40, 5472–5475 (1989).
23. O. Thual and S. Fauve, J. Phys. (France), 49, 1829–1833 (1988).
24. A.M. Turing, Philosopical transactions of the Royal Society of London, B 357, 37–72 (1952).
25. G.H. Gunaratne, Q. Ouyang, and H.L. Swinney, Phys. Rev. E., 50, 2802–2820 (1994).
26. E. Ciaramella, M. Tamburrini, and E. Santamato, Appl. Phys. Lett., 63, 1604–1606 (1993).
27. T. Honda and H. Matsumoto, Opt. Lett., 20, 1755–1757 (1995).
28. G.S. McDonald and W.J. Firth, J. Opt. Soc. Am., B 7, 1328–1335 (1990).
29. G.S. McDonald and W.J. Firth, J. Mod. Opt., 37, 613–626 (1990).
30. M. Kreuzer, Thesis, (TH Darmstadt, 1994).
31. R. Neubecker and T. Tschudi, J. Mod. Opt., 41, 885–906 (1994).
32. J.Y. Bigot, A. Daunois, and P. Mandel, Phys. Lett. A, 123, 123–127 (1987).
33. B. Segard, J. Zemmouri, and B. Macke, Opt. Commun., 63, 339–343 (1987).
34. F. Mitschke, C. Boden, W. Lange, and P. Mandel, Opt. Commun., 71, 385–392 (1989).